SLAC-PUB-9280
July 2002

A Very High Resolution Optical Transition Radiation Beam Profile Monitor*

Marc Ross, Scott Anderson, Josef Frisch, Keith Jobe, Douglas McCormick, Bobby McKee, Janice Nelson, Tonee Smith

Stanford Linear Accelerator Center, Menlo Park, CA, 94025, USA

Hitoshi Hayano, Takashi Naito, Nobuhiro Terunuma

High Energy Accelerator Research Organization, Tsukuba, Ibaraki 305-080,1 Japan

Abstract. We have constructed and tested a 2 um resolution beam profile monitor based on optical transition radiation (OTR). Theoretical studies of OTR [1] show that extremely high resolution, of the order of the wavelength of the light detected, is possible. Such high-resolution single pulse profile monitors will be very useful for future free electron laser and linear collider projects. Using the very low emittance 1.3 GeV electron beam at the KEK Accelerator Test Facility (ATF) [2] (1.4nm εx x 15pm εy), we have imaged transition radiation from 5 micron σ beam spots. Our test device consisted of a finely polished target, a thin fused silica window, a 35 mm working distance microscope objective (5x and 10x) and a triggered CCD camera. A wire scanner located near the target is used to verify the profile monitor performance. In this paper we report results of beam tests.

INTRODUCTION

Measurement of the low emittance beams produced by a linear collider damping ring require a device that can image beam spots as small as 5 microns. Small beam sizes are often measured using wire scanners [3], requiring many machine pulses, often with an over-estimation of the beam size due to beam position and intensity jitter [4]. In addition, wire scanner measurements can take up to half a minute to complete. An optical beam spot size monitor based on OTR can be used to record images from single pulses and, in principle, have a resolution of about one micron.

Optical beam size monitors are typically based on fluorescent screens, OTR or synchrotron radiation. Fluorescent screens are practical when $\sigma > 30$ μm [5]. Beam spots with $\sigma < 30$ μm are difficult to measure due to effects from phosphor grain size and phosphor transparency, which gives rise to depth of field problems. Synchrotron radiation from a bend magnet is confined to a cone of opening angle $1/\gamma$ (< 0.5 mrad at the ATF where $E_b \sim 1.3$ GeV). The diffraction-limited resolution due to this opening angle is typically much larger than the beam size for typical linear collider damping ring parameters.

Transition radiation is produced when relativistic charged particles transit through the surface of a conductor. The backward directed radiation is emitted from the surface at an angle equal to the angle made by the incoming beam. The radiation is emitted primarily in a cone with an opening angle of about 1 mrad for 1.3 GeV. With this opening angle, the expected resolution limit due to diffraction might be expected to be similar to that for synchrotron radiation. However, the transition radiation distribution has large tails that emerge at greater angles, the key feature that makes a very high-resolution OTR monitor possible. Because the radiation is primarily forward-directed, the large angle radiation must be efficiently collected, requiring an optical system that has a larger numerical aperture (by approximately a factor of 2) than would be needed for a diffuse light source.

Work supported in part by the Department of Energy contract DE-AC03-76SF00515.
Presented at the 10th Beam Instrumentation Workshop (BIW 02), Upton, New York, 5/6/2002 - 5/9/2002

OTR beam profile monitors will be used in the linear collider or in an FEL light source to check the emittance and beam optics match. Linear colliders are designed with large aspect ratio (σx/σy), 'flat' beams. The monitor will be used as part of the skew correction process in which *x* - *y* coupling is corrected by a sequence of skew quad magnets. Simulations show that even with ideal skew correction systems, the presence of small, nominal wire scanner errors can make tuning algorithms unstable [6]. OTR has the promise of reducing the error on the beam tilt measurement.

Some controversy exists over the ultimate resolution of an OTR profile monitor[1]. Tests reported here include a search for the minimum observable beam spot. A 5.5 um high, ~200 um wide beam stripe was generated and clearly imaged.

The OTR can be susceptible to beam related damage when high charge density beams impinge on its polished surface. Since the wide image mentioned above was quite faint, we made a much smaller beam spot and subsequently, over the course of a few minutes operation at 0.75 Hz, noticed damage on the surface of the mirror. The damage quickly ruined the mirror to such an extent that further studies of resolution were not possible.

The design goal of the OTR monitor in the ATF extraction line is intended to measure a (σx, σy) ~ (50, 5) micron beam with better than 10% resolution. The monitor uses a mechanically polished mirror target approximately 500 um thick with an entire field of view of 360 x 250 um. In this paper we discuss the design, installation, and beam testing of an OTR beam size monitor in the ATF extraction line. We also report tests of several different target materials: Cu, Be, glassy Carbon, Ti and Si.

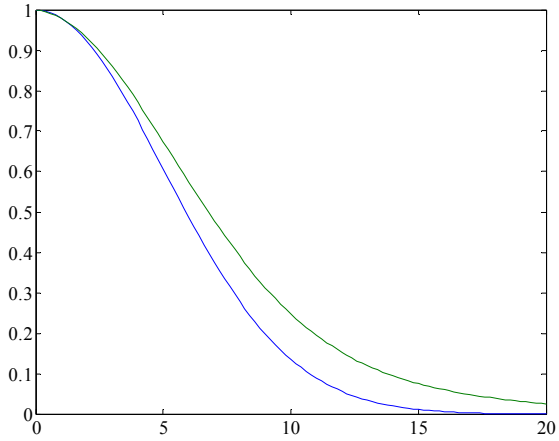

Figure 1. A calculated 5 micron spot (lower curve) and its predicted image (top curve).

OPTICS

The resolution required to measure the minimum expected beam size in the ATF with a 10% accuracy is about 2 um. Unfortunately, imaging with an ideal lens through a thick vacuum window introduces spherical and chromatic aberrations. Commercial microscope objectives are not compatible with high vacuum systems, and design and construction of custom vacuum compatible optics is time consuming and expensive.

While it is possible to design a lens to compensate for the aberration caused by a window we decided to use a commercial microscope objective to avoid the cost of a custom design. ZEMAX [7] calculations indicated that using a thin (<1 mm) window would reduce the effect of the aberrations to within our design tolerances. Mechanical calculations show that the distortion due to vacuum pressure is acceptable (<λ/4) for a fused silica window with a diameter of <7 mm.

To meet the high numerical aperture requirements, a long working distance microscope objective manufactured by Mitutoyo was chosen. Their 5X objective has a numerical aperture of 0.14, with a focal length of 40 mm and working distance of 34 mm. The lens is designed for use at infinite conjugate ratio (i.e. focuses a point to a parallel beam), and gives a depth of focus of approximately ± 7 um. The lens has a specified resolving power of 2um, corresponding to diffraction-limited performance. This is roughly equivalent to a resolution of 1 um sigma.

Figure 2 shows a schematic of the OTR monitor. The lens is mounted to a 200 mm tube lens adapter and a 200mm tube that mounts directly to a C-mount camera. The objective and adapter provide a magnification of 5X

onto the camera, which is reasonable for a camera pixel size of ~10 μm. For some tests a 10X lens with a numerical aperture of 0.28, but otherwise similar design, was used.

Transition radiation from a target that is not normal to the electron beam is emitted in a direction corresponding to a geometric reflection of the incident beam angle. The microscope axis must therefore be aligned at an angle to the target, resulting in a change in focal depth with position on the target. Tilting the image plane of the camera can in principal compensate this tilted object plane, however for our parameters this was impractical. Instead we oriented the target so that the small vertical spot dimension was aligned with the tilt angle, and accepted a very narrow field of view. The target angle relative to the beam was chosen to be 20 degrees, the smallest allowed by mechanical constraints.

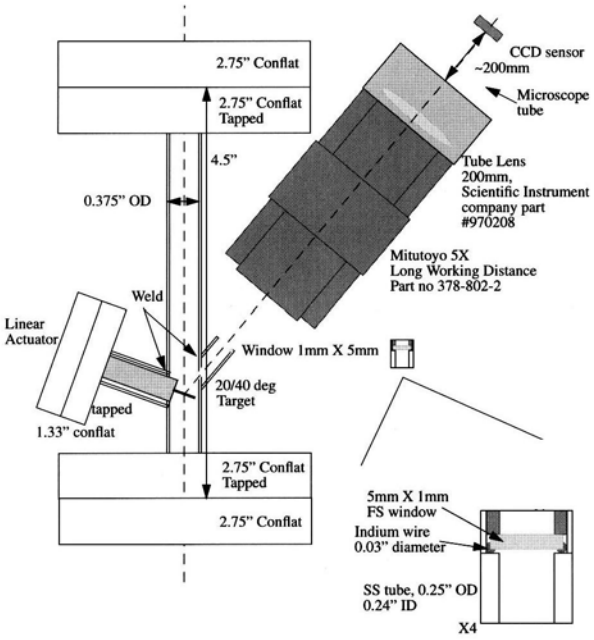

FIGURE 2. Schematic drawing of the OTR monitor with the beam entering from the top of the view. This shows the lens setup of the camera telescope.

The optical system should image a point source to a spot with a sigma of ~1 micron; however transition radiation is forward directed, resulting in poorer resolution than for a uniform source. A numerical calculation using the predicted OTR distribution shows that a 5 um sigma spot will be broadened by <10% by the convolution of the transition radiation and diffraction (see figure 1).

MECHANICAL DESIGN

There are two critical mechanical design issues: (1) placing the microscope objective within its working distance, and (2) sealing the thin fused silica window in the body of the device without distorting it.

In order to have the objective within its working distance, the beam pipe would have to be about 1 cm in diameter. Even with the small beams in the ATF extraction line, 1 cm was determined to be too small and a pipe mover was developed, located in the background of figure 3.

The window port was machined to accept an indium seal, and its bore was threaded to accept a screw plug for compressing the window between an O-ring and the indium seal. This seal proved to be problematic and required careful installation to make it vacuum tight.

The target is inserted and removed by a pneumatic actuator that consists of a thin rod to which the target is attached with screws. To make the target insertion reproducible, a stainless steel ball welded on the end of the actuator is designed to seat into a titanium conical receptacle in the wall of the device.

The microscope objective is mounted to an optical translation stage that is remotely controllable using a micro-stepper motor. The stage is used to control the camera focus.

BEAM STUDIES

The purpose of the beam studies was to test the OTR monitor resolution and to begin comparing beam emittance estimates made with the monitor and the nearby wire scanners. First, operational parameters such as focus, depth of field and calibration were tested and a 'minimum' beam size measurement was done. Following that, several emittance measurements were made using the nominal ATF beam.

An alignment test stand was prepared to position the apparatus such that an laser could be shown down the beam pipe onto the target. The target was rotated by loosening the vacuum flange of the actuator and rotating it until the laser light projected out of the center of the window. The target was scribed with four lines using a razor blade to provide position information. Using the laser light, the camera was adjusted until two of the vertical lines were on the edges of the field of view. The apparatus was then installed in the ATF extraction line near one of the wire scanners.

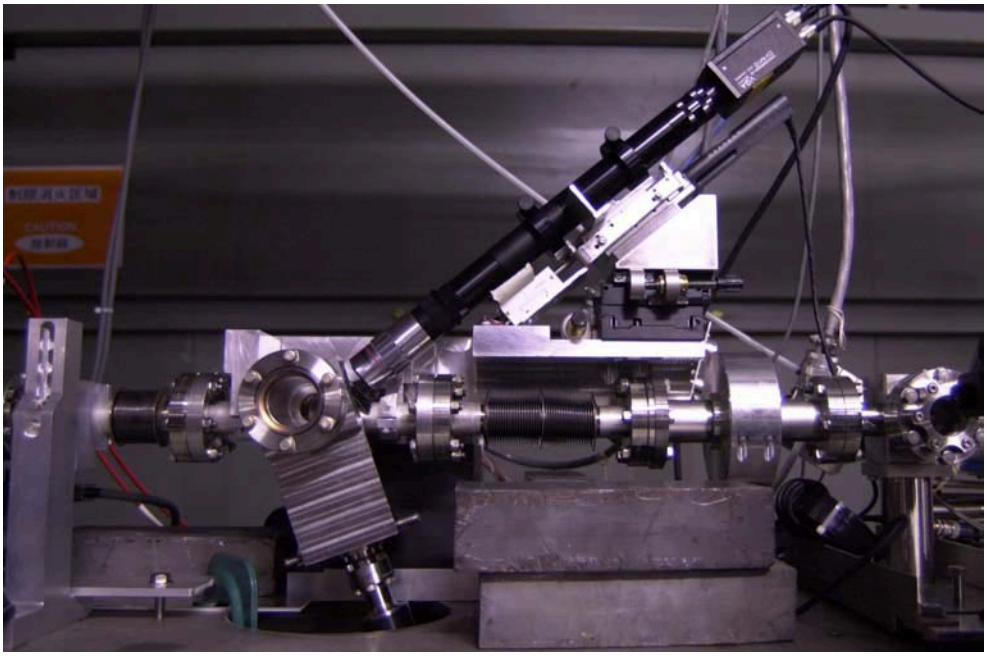

Figure 3. The OTR monitor installed in the ATF extraction line.

The extraction line was setup with normal beam optics, and the Cu target was inserted. The light spot was quickly found, steered to the center of the screen, and digitized to obtain FWHM size in digitizer channels.

The camera focus was checked by using a stepper motor to move the camera stage. The depth of focus scan clearly indicated that the beam had to be kept within a ± 25 micron vertical window in order to avoid affecting the beam size measurement due to out of focus effects.

The calibration of digitizer channels to microns in x was calculated by positioning the beam over each of two vertical scribe lines that are 0.5 mm apart. To calculate the calibration for the vertical channels, a reference BPM orbit was saved and both nearby wire scanner y wires were scanned and their centroids noted. Then a corrector was moved by a known amount, another BPM orbit was saved, and the wires scanned again. By plotting the wire scanner centroid and BPM position changes against the predicted changes based on the optics model, the change in the position at the OTR was calculated. This distance was divided by the change between the centroids of the digitized spots (in channels) to obtain the y calibration in microns/channel. The vertical calibration was calculated to be 1.06 μm/channel and the horizontal to be 1.12 microns/channel, accurate to 2%.

For the resolution test, the optics in the extraction line were adjusted to produce a calculated beam size of 1 micron at the OTR. The quadrupole values were implemented in stages to prevent the beam moving out of the camera field of view. At each stage, the beam image was digitized and the *y* spot size was recorded. Over the course of the scan, an increased tilt was observed in the beam spot; several attempts were made to correct this with skew quads, with only partial success. As the *y* spot size was reduced (and the *x* spot size greatly increased), the available light intensity became so small that optimization tuning was difficult as the spot was too dim to see.

At the smallest vertical beam size, we were unable to find the maximum resolution of the device due to decreased light and poor signal to noise ratio. The smallest *y* spot size measurement was approximately 5.5 microns. Figure 4 below shows OTR images as captured by the digitizer software with projections in *x* and *y*.

Next, the beryllium target was installed in the OTR and the nominal optics was implemented in the extraction line. The measurements from the quadrupole scans in the normal optics compare well to five-wire emittance measurements taken after the quadrupole scans were completed. The results are displayed in the Table 1. The slight discrepancies in the results are possibly due to the fact that the five-wire and quadrupole scan measurements were not taken with precisely the same optics setup: while both setups started with the nominal extraction line optics, the extraction line dispersion was measured and corrected in each case to produce two possibly slightly different optics starting points. The quadrupole emittance measurements take into account the dispersion at each monitor, the wire sizes of MW3X and MW4X and the estimated resolution error of the OTR. The OTR is estimated to have a resolution of 2-3 μm and a 2 μm addition in quadrature was used for the quad emittance calculation.

Table 1. Vertical emittance measurements from OTR, MW3X and MW4X quad scans and five-wire emittance measurement.

Device	ε_y
OTR	$2.741 \times 10^{-11} +/- 8.867 \times 10^{-13}$ m
OTR, tilt corrected	$1.779 \times 10^{-11} +- 1.435 \times 10^{-12}$ m
Wire Scanner 3 (upstream)	$2.222 \times 10^{-11} +/- 1.165 \times 10^{-12}$ m
Wire Scanner 4 (downstream)	$2.789 \times 10^{-11} +/- 9.029 \times 10^{-13}$ m
Five-wire	$2.55 \times 10^{-11} +/- 1.2 \times 10^{-12}$ m

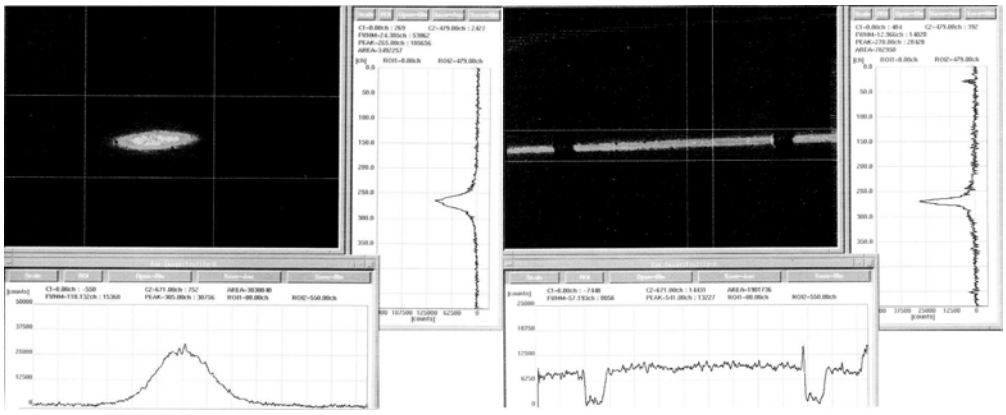

Figure 4. Beam spot as seen by Be OTR with normal extraction line optics (left image). The *y* FWHM is 24 channels, which corresponds to a *y* sigma of about 10 μm. Beam spot at OTR with "2 μm" optics loaded (right image). Here the *y* FWHM is 12.9 channels or about 5.8 μm. The gaps in the image are caused by the scribe marks used for calibration.

The wire and uncorrected OTR emittance measurements don't take into account the tilt of the beam, which varied between two and ten degrees for the OTR during the quad scan, and by some unknown amount for the wire scanners for both the quad scan and the five-wire measurements. If the tilt is taken into account for the OTR measurements, the emittance measured by the OTR is reduced by 40%.

Figure 5. Beam on *Be* target before (left) and after (right) five minutes at 5.5 x10^{10} e^-/bunch train.

TARGET MATERIAL TESTS

The 'energy to break' is defined in equation 1 as the energy at which the material strength is exceeded due to thermal induced mechanical stress:

$$ETB = 2*(1-\mu)*\frac{\mathrm{UTS}*\mathrm{C}}{\alpha*\mathrm{E}}\ \mathrm{(J/g)} \qquad (1)$$

where μ is Poisson's Ratio, UTS is the Ultimate Tensile Strength, C is the heat capacity, α is the coefficient of thermal expansion and E is Young's modulus. For a gaussian distribution of N particles with rms σ_r, the normalized probability distribution is p(r):

$$\mathrm{p(r)} = \frac{\mathrm{N}}{2\pi\sigma_{\mathrm{r}}^{2}}\mathrm{e}^{-\frac{\mathrm{r}^2}{2\sigma_{\mathrm{r}}^2}}$$

For energy deposition, $\frac{\mathrm{dE}}{\mathrm{dx}}$, in units of $\frac{\mathrm{MeV}-\mathrm{cm}^2}{\mathrm{g}}$, q = the charge per electron, σ_r in meters and the peak energy deposition is ΔE_{peak} (in units of J/g):

$$\Delta E_{peak} = 100q\frac{dE}{dx}\frac{N}{2\pi\sigma_r^2}\ \mathrm{(J/g)}$$

The temperature rise is $\Delta\mathrm{T(r)}$:

$$\Delta\mathrm{T(r)} = \frac{23.9}{\mathrm{C}}\mathrm{q}\frac{\mathrm{dE}}{\mathrm{dx}}\frac{\mathrm{N}}{2\pi\sigma_{\mathrm{r}}^2}\mathrm{e}^{-\frac{\mathrm{r}^2}{2\sigma_{\mathrm{r}}^2}}\ (^{\mathrm{o}}\mathrm{C})\ \text{ and }\ \Delta\mathrm{T}_{\mathrm{peak}} = \frac{23.9}{\mathrm{C}}\mathrm{q}\frac{\mathrm{dE}}{\mathrm{dx}}\frac{\mathrm{N}}{2\pi\sigma_{\mathrm{r}}^2}\ (^{\mathrm{o}}\mathrm{C})$$

where C = the heat capacity in units of cal/(g-^{o}C)

Table 2 summarizes the material damage tests. To test the damage threshold of the beryllium target, the extraction line optics were set up to deliver a 13 by 10 μm of 8 x 10^9 electrons per beam pulse at the OTR. The beam was left on the target over the course of thirty minutes with no damage seen using both the normal x5 lens and a x10 lens. This result is in direct contrast to the damage seen on the copper targets at the same intensities and small spot sizes. Since no damage occurred at the lower current in single bunch mode, the beryllium target was then subjected to 5.5 x10^{10} electrons in 20 bunches per pulse, with the same small spot optics. At this higher intensity, damage occurred after five minutes. Figure 5 shows the OTR beam image at the beginning of this high current destruction test (left image) and the OTR beam image after five minutes (right image). The beryllium target shows noticeable

damage that alters the image and would compromise a beam size measurement. The glassy carbon II target was not subjected to a high current destruction test due to time limitations.

Table 2: Target material damage test results. The table shows what was observed (D: Damaged, ND: No Damage, I: Inconclusive) and the estimated energy deposition (J/gm). All tests were done with a 1.5 Hz repetition rate.

Target Material	Energy to Break (J/gm)	Single bunch 7.5e9 20x12um	Single bunch 8.9e9 13x10um	Multibunch 5.5e10 20x15um	Multibunch 2.9e10 43x34um	Multibunch 2.8e10 16x10um
Cu	98	D; 118 J/gm				
Be	484	ND; 150	ND; 315	D; 845		
C (II)	580-735	ND; 140				
Si	(?)	ND; 130			ND; 91	
Ti	710	ND; 119				I; 670

The sequence of figures, (6a-c), show the progression of damage to the polished Cu surface. At first, a smooth image is seen, shortly after steering the finely focused spot onto a fresh surface. The features above the spot in Figure 6a are from earlier tests. Then, after 3-4 minutes, (Figure 6b), a wrinkled looking image begins to emerge followed by, (Figure 6c), substantially wrinkling. At that point, no further obvious signs of damage appeared after about ½ hour of operation. At the final stage of damage, the target must have some vertical features or relief, because it became quite difficult to determine when the image was in focus. Different features came into focus at different lens stage positions. Using these expressions a peak deposited energy of 67 J/g and a temperature rise of 174 deg C is expected in the copper for a round spot, beam size σ_{xy} = 20 microns and N = 0.75e10. In the experiment described here, the beam size σ_{xy} ~ 20 x 12 microns raises the energy deposition by 67% to 112 J/g and the temperature to 290 deg C. While this is well below the melting point of copper (1083 deg C), it is above the temperature where local pressure in the bulk material causes plastic deformation, estimated to be about 180 deg C. The thermal diffusion constant alpha (alpha^2 = 1.16 cm^2/s) is high enough such that at 1 Hz we don't expect any noticeable temperature build up.

The damage to beryllium at 5.5 x10^{10} electrons is not surprising. The energy deposited was roughly 850 J/g, which is well above the energy to break of 484 J/g for beryllium [8]. Glassy carbon type II's energy to break is in the range of 580-735J/g (assuming a 0.29-0.1 μ) and it showed no damage at the single bunch currents up to 0.8 x10^{10} in the small spot optics. The results of the tests are summarized in table 2.

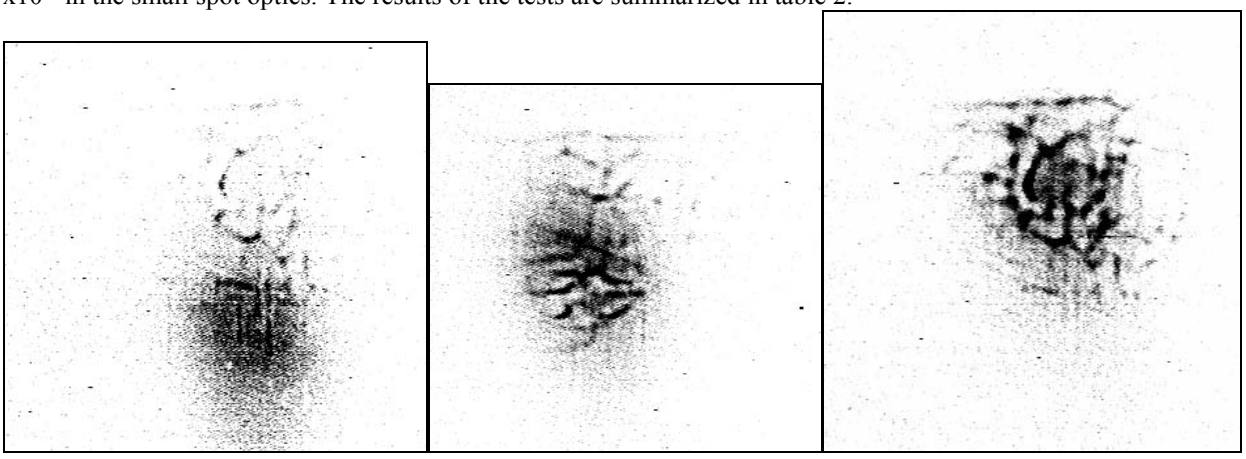

Figure 6(a): Negative image of a 20 x 12 um (σ_x, σ_y) beam spot before damage. Some damage is visible above the beam spot from earlier tests. The figure shows the entire field of view (360 x 250 microns). Figure 6(b): Taken a few minutes after the onset of damage. Figure 6(c): Showing damage at a more advanced stage.

CONCLUSIONS

The OTR was successful in measuring the size and emittance of the beam in the ATF extraction line using two different target materials, beryllium and glassy carbon II. The measurements of beam size versus the predicted size from the five-wire emittance calculation agreed well in the vertical plane and were within 15% in the horizontal plane. The quadrupole scan emittance measurement at the OTR agrees well with the simultaneous scanner downstream wire scanner measurement and with a subsequent five-wire scan emittance measurement. The OTR and the nearby upstream scanner measurements differ by 25%, far outside the error. The tilt of the beam at each of the measuring devices was not corrected online in any of the measurements in this experiment. When the skew was corrected offline for the OTR, the resulting emittance was reduced by 40%, well below the uncorrected wire scanner results. It is presumed that correcting for the beam tilt at the wires would similarly reduce the wire scanner emittance results.

The measurements completed in these experiments suggest that the OTR could be a valuable tool for measuring the beam size and emittance parameters from the ATF damping ring. Given its apparent resolution and its ability to take horizontal and vertical beam size measurements in one beam pulse and to take many measurements quickly, the OTR should be able to measure the beam emittance with high statistics, giving a low error and a good understanding of emittance jitter. Multiple OTR measuring devices located near the wire scanners in the ATF extraction line would be a definitive test of the OTR as a beam emittance diagnostic device.

REFERENCES

* Work supported by Department of Energy, Contract DE-AC03-76SF00515

1 M. Castellano, V.A. Verzilov, Phys. Rev. ST Accel. Beams 1, 062801 (1998)
2 T.Okugi et al., Phys. Rev. ST Accel. Beams 2, 022801 (1999)
3 H. Hayano, 'Wire scanners for small emittance beam measurement in ATF', Linac 2000.
4 M.C. Ross, 'Wire scanner systems for beam size and emittance measurements at SLC', Second Accelerator Instrumentation Workshop (1990).
5 F. Decker, 'Beam Size Measurement at High Radiation Levels', PAC 1991 (SLAC-PUB-5481).
6 M. Woodley, KEK Accelerator Test Facility Internal Note 99-07, http://atfweb.kek.jp/atf/Reports/ATF-99-07.pdf.
7 http://www.optima-research.com/Software/Optical/Zemax/
8 Private Communication. Material damage calculation from John Sheppard, which is used in explaining damage to e+ target materials.